Published in final edited form as:
*Ann Thorac Surg*. 2012 June ; 93(6): 1964–1971. doi:10.1016/j.athoracsur.2012.03.001.

# Patient-specific finite element based analysis of ventricular myofiber stress after Coapsys: Importance of residual stress.

**Richard Carrick, BS**[1], **Liang Ge, PhD**[2,3,5], **Lik Chuan Lee, PhD**[2,3,5], **Zhihong Zhang, MS**[5], **Rakesh Mishra**[4,5], **Leon Axel, MD, PhD**[6], **Julius M. Guccione, PhD**[2,3,5], **Eugene A. Grossi, MD**[6,7], and **Mark B. Ratcliffe, MD**[2,3,5]

[1]College of Medicine of the University of Vermont, University of California, San Francisco, California

[2]Departments of Surgery, University of California, San Francisco, California

[3]Departments of Bioengineering, University of California, San Francisco, California

[4]Departments of Medicine, University of California, San Francisco, California

[5]Veterans Affairs Medical Center, San Francisco, California

[6]Departments of Cardiothoracic Surgery and Radiology, New York University, New York

[7]New York Harbor Veterans Affairs Medical Center

## Abstract

**Background—**We sought to determine regional myofiber stress after Coapsys device (Myocor, Inc., Maple Grove, Minnesota) implantation using a finite element (FE) model of the left ventricle (LV). Chronic ischemic mitral regurgitation (CIMR) is due to LV remodeling after postero-lateral myocardial infarction. The Coapsys device consists of a single trans-LV chord placed below the mitral valve such that when tensioned it alters LV shape and decreases CIMR.

**Methods—**FE models of the LV were based on magnetic resonance images (MRI) obtained before (PRE-OP) and after (POST-OP) CABG + Coapsys in a single patient. To determine the effect of Coapsys and LV pre-stress, virtual Coapsys (VIRTUAL-COAPSYS) was performed on the PRE-OP model. Diastolic and systolic material parameters in the PRE-OP, POST-OP and VIRTUAL-COAPSYS were adjusted so that model LV volume agreed with MRI data. CIMR was abolished in the post-op models. In each case, myofiber stress and pump function were calculated.

**Results—**Both POST-OP and VIRTUAL-COAPSYS shifted end-systolic (ES) and end diastolic (ED) pressure volume relationships (PVR) to the left. As a consequence and because CIMR was reduced after Coapsys, pump function was unchanged. Coapsys decreased myofiber stress at ED and ES in both the remote and infarct regions of the myocardium. However, knowledge of Coapsys and LV pre-stress was necessary for accurate calculation of LV myofiber stress especially in the remote zone.



Corresponding Author: Mark Ratcliffe, Surgical Service (112), San Francisco Veterans Affairs Medical Center, 4150 Clement Street, San Francisco, California 94121. Telephone: (415) 221-4810 x 2962. FAX: (415) 750-2181. mark.ratcliffe@va.gov.

**Conclusions—**Coapsys decreases myofiber stress at ED and ES. The improvement in myofiber stress may contribute to the long term effect of Coapsys on LV remodeling.

### Keywords

Myocardial Infarction; Remodeling; Mitral Valve; Mitral Regurgitation; Mitral Repair; Finite Element; Stress

## Introduction

Most surgeons perform reduction annuloplasty to treat chronic ischemic mitral regurgitation (CIMR) at the time of coronary bypass (CABG). However, repair of CIMR with reduction annuloplasty fails in up to 30% of patients. [1-5] Those failures occur in large part because of continued displacement of the posterior papillary muscle (PPM) [1] since annuloplasty is able to correct mitral regurgitation but does not stop left ventricular (LV) remodeling.

As a consequence, a number of ‘sub-valvular’ procedures that relocate the PPM have been proposed. Examples include a suture placed between the PPM and the right posterior mitral annulus as proposed by Kron [6], a suture between the PPM and the right fibrous trigone of the anterior mitral annulus as described by Langer et al (‘String-1’) [7, 8], or between the lateral and anterior LV walls as is the case with the Coapsys LV reshaping device. [9]

The Coapsys device consists of a single trans-LV chord placed below the mitral valve such that when tensioned it alters LV shape and decreases CIMR. Implantation does not require cardiopulmonary bypass. As previously reported [10], Coapsys reshapes the ventricle, decreases the septo-lateral dimension of the mitral valve, decreases CIMR and is associated with continued reduction in LV size. [11] The Coapsys device is of particular interest because the recently presented RESTOR-MV Trial found a survival advantage of CABG +Coapsys over Control (CABG+reduction annuloplasty) at 2 years (87% vs 77%; p=0.038). [12]

Finite element (FE) simulation of cardiac surgical procedures and devices is becoming more common. Specifically, simulations of passive LV constraint [13] the Dor procedure [14] and cardiac resynchronization therapy [15] have been performed. Furthermore, we have recently demonstrated that the magnitude of stress calculated with the Young-Laplace law is very different than stress in the myofiber and cross-myofiber directions calculated with the finite element method. [16]

In the current study, we constructed FE models of the LV that were based on magnetic resonance images (MRI) obtained before (Pre) and after (Post) CABG + Coapsys device in a single patient. We tested the hypotheses that Coapsys reduces regional LV myofiber stress.

## Material and Methods

### Coapsys procedure

The Coapsys procedure was performed in a randomized clinical trial for patients with moderate or severe CIMR. [12] This study was performed under a New York Harbor Veterans Affairs Medical Center (NYHVAMC) Institutional Review Board (IRB) approved protocol. Subsequent analysis of radiographic images obtained on Coapsys patients was also approved by the NYHVAMC IRB. Hemodynamic monitoring during the procedure was performed with radial arterial and Swan Ganz catheters. Figure 1 shows the Coapsys device.

### MRI

A series of long and short-axis images of the heart were obtained using cine gradient echo imaging (Figure 2). MRI data acquisition was triggered by the QRS complex of the electrocardiogram. Delayed enhancement images were obtained approximately 10-15 minutes after intravenous injection of 0.15 mmol/Kg gadolinium-DTPA.

### Image Analysis

A customized program (iContours, Liang Ge, Cardiac Biomechanics Lab, San Francisco, CA) based on the medical image processing environment Mevislab (v 2.1, Mevislab, Bremen, DE) was used to contour the endocardial and epicardial surfaces of the LV. End diastole (ED) and end systole (ES) were defined as the images with the maximum and minimum cross sectional area, respectively.

### FE model of the LV; Overview

FE models of the LV was created based on pre- and post-operative MRI images (PRE-OP and POST-OP models respectively) (Figure 3). Please note that the POST-OP model was based on the unrealistic assumption that there is zero stress in the Coapsys LV chord and in the LV wall at early diastolic filling. In order to account for device and LV pre-stress, virtual Coapsys was performed on the PRE-OP model (VIRTUAL-COAPSYS; Figure 4). In that regard, VIRTUAL-COAPSYS:ACUTE shows the acute mechanical effect of the Coapsys device while VIRTUAL-COAPSYS:SUBACUTE shows the effect after systolic material properties are adjusted for agreement with post-operative MRI data.

Endocardial and epicardial surfaces were created from LV contours (Rapidform; INUS Technology, Inc, Sunnyvale, CA). The space between the surfaces was filled with 8-node trilinear brick elements to generate a volumetric mesh that was 3 elements thick (Truegrid; XYZ Scientific Applications, Inc, Livermore, CA). Based on the MRI delayed enhancement images, an infarct zone was created in the infero-lateral wall of the LV. The remainder of the LV was designated the remote zone.

Cardiac myofiber angles at the epicardium and endocardium were assigned to be −60 degrees and 60 degrees respectively (counterclockwise positive when viewed from the epicardium) with respect to the circumferential direction, with a linear variation across the LV wall.

### Material properties

Nearly incompressible, transversely isotropic, hyperelastic constitutive laws for passive and active myocardium were implemented with a user-defined material subroutine in the explicit FE solver, LS-DYNA (Livermore Software Technology Corporation, Livermore, CA), as previously described. [17] Myocardial material parameters (passive myocardial stiffness parameter ‘C’ and active myofiber contractility parameter ‘Tmax’) were estimated by comparing experimentally measured and computationally derived LV volumes at ED and ES respectively. Manual iteration was used rather than formal optimization [18] and iteration was continued until the difference between experimental and computational values was within 1%. Separate material parameters were determined for PRE-OP, POST-OP and VIRTUAL-COAPSYS models. The infarct region was assigned a passive stiffness 10 times greater than the remote zone. The infarct zone had no contractility.

### Loading conditions and constraints

The basal nodes of the LV were constrained in the z-direction, with the exception of the basal nodes of the epicardium which were fully constrained in all directions. The

endocardial wall was loaded to the measured in vivo end-diastolic and end-systolic LV pressures.

### Finite element model of the Coapsys device

A model of the Coapsys device that included the trans-LV chord, and anterior and posterior pads was developed. The two posterior pads were connected by a rigid beam element attached to the center of pads. The trans-LV chord of the Coapsys device was modeled as a discrete beam element (*MAT_071). The chord was assigned a Young's modulus of $1*10^6$ kPa to eliminate stretching.

The Coapsys model was initially used in the POST-OP model. In that case, however, the trans-LV chord and myocardium around the anterior and posterior pads was assumed to be stress free. A unique feature of *MAT_071 is that an axial tension can be specified for each beam element and this axial tension could mechanically pull the two ends of each element together. Using this feature of *MAT_071, a VIRTUAL-COAPSYS procedure was performed on the unloaded PRE-OP model. The trans-LV chord was virtually tightened until the length of the trans-LV chord was the same as in the POST-OP model. Tightening of the trans-LV chord caused pre-stress to the trans-LV chord and myocardium around the anterior and posterior pads.

In each case, simulation of LV diastole and systole was performed as previously described. [19] The relationship between stroke volume (SV) and LV pressure at ED ($P_{ED}$) (Starling) relationship was calculated from diastolic and systolic pressure-volume regressions using the following equation that relates arterial elastance, $E_A$, to stroke volume [20]

$$SV = \frac{V_{ED} - V_0}{1 + E_A / E_{ES}} \quad (1)$$

where $SV$ is the forward stroke volume, $V_{ED}$ is the LV volume at ED, $V_0$ is the volume intercept and $E_{ES}$ is the slope of end-systolic ESPVR.

In the PRE-OP model, forward SV was calculated by subtracting the regurgitant volume and regurgitant fraction was assumed to be constant for all pressure volume loops. $E_A$ was assumed to be unchanged after the Coapsys procedure. [21]

### Statistical analysis

Midwall myofiber stress and strain were averaged over all elements in each LV region. The values presented are the average stress (or strain) + standard deviation in each region.

A single finite element model based on a single patient was employed. The results obtained are not stochastic and statistical tests were therefore not appropriate. P values are therefore not reported.

## Results

### Clinical data

The single patient was a 58 year old man with worsening dyspnea and chest tightness on exertion. Echocardiography showed severe MR (an effective regurgitant orifice of $0.4cm^2$) and a LVED dimension of 6.3cm. Cardiac catheterization showed a mild left main stenosis, high grade stenosis of the circumflex and occlusion of the right coronary artery.

The patient underwent MRI six weeks before CABG and Coapsys implantation (Figure 2A). Pre-operative MRI showed a dilated LV (Table 1) with reduced ejection fraction = 29.7%. There was akinesis and hyper-enhancement of the inferior and lateral walls. There was moderate to severe mitral regurgitation (regurgitant fraction of 30%).

The patient underwent CABG and mitral valve repair via ventricular reshaping using the Coapsys device. Intraoperative data is included in Table 2. Systolic arterial and diastolic pulmonary pressures were used as measures of $P_{ES}$ and $P_{ED}$ in all three FE simulations. The patient underwent MRI two weeks after CABG and Coapsys implantation (Figure 2B).

### Finite element simulation: Comparison with clinical data

Table 1 shows the comparison between input data and FE model results. The passive and active material properties for the baseline and post-surgery LV wall are shown in Table 3. The passive material property was almost identical between the PRE-OP and the POST-OP models. Surprisingly, however, the POST-OP $T_{max}$ is lower than the PRE-OP $T_{max}$.

### Finite element simulation: Effect of Coapsys on ESPVR and EDPVR

Figure 5 shows the EDPVR and ESPVR for PRE-OP, POST-OP and VIRTUAL-COAPSYS (ACUTE and SUBACUTE) numerical experiments. Compared with the PRE-OP case, POST-OP and VIRTUAL-COAPSYS caused leftward shift of both ED and ESPVR. VIRTUAL-COAPSYS:ACUTE was associated with a slightly greater leftward shift of ESPVR and POST-OP was associated with a slightly less shift in EDPVR.

### Pump function/Starling relationship

Figure 6 shows Starling curves calculated from the four numerical experiments. The VIRTUAL-COAPSYS:ACUTE and POST-OP Starling curves are similar and lie slightly above and to the left of the VIRTUAL-COAPSYS:SUBACUTE and PRE-OP Starling curves.

### Myofiber stress

Figure 7 shows average end-diastolic and end-systolic myofiber stress in LV regions for all four numerical experiments. End-diastolic and end-systolic myofiber stress was not changed in the POST-OP model in the remote zone. However, in both the VIRTUAL-COAPSYS:ACUTE and VIRTUAL-COAPSYS:SUBACUTE models and in the POST-OP model in the infarct zone myofiber stress was reduced at both ED and ES. The ES fiber stress in the VIRTUAL-COAPSYS models was reduced by 18% and 35% in remote and infarct regions, respectively. The corresponding ED stress reduction was 28% and 42%.

The axial force on the subvavular chord predicted by the VIRTUAL-COAPSYS:SUBACUTE was 4.64 N at ED and 18.03 N at ES. The corresponding predicted force by the VIRTUAL-COAPSYS:Acute and POST-OP cases were 5.72 and 22.91 N for ED and ES respectively. The ES myofiber stresses distribution predicted by the PRE-OP and VIRTUAL-COAPSYS:SUBACUTE cases are shown in Figure 8.

## Comment

The principal finding of this study is that Coapsys decreases myofiber stress in both the remote and infarct regions of the myocardium at ED and ES. However, knowledge of pre-stress in the trans-LV chord and myocardium around the anterior and posterior pads was necessary for accurate calculation of LV myofiber stress especially in the remote zone.

### Patient specific modeling

Patient specific computational modeling can aid diagnosis and optimize design of operations and devices for the treatment of cardiovascular disease. As above, finite element based analysis of operations and devices to treat heart failure including passive LV constraint [13], the Dor procedure [14] and cardiac resynchronization therapy [15] has been particularly useful. In the present case, patient-specific modeling has the potential to optimize Coapsys chord tension and the location of epicardial anchors, factors that have previously been determined empirically at the time of surgery

### Reduction in fiber stress

The trans-ventricular strut of the Coapsys device becomes a structural element of the LV that, when applied as described above, is under tension at both end diastole and end systole. As demonstrated by our finite element based analysis, Coapsys causes a reduction in both diastolic and systolic ventricular fiber stress. Our results are in line with those of McCarthy and colleagues who found that the Myosplint type trans-ventricular strut reduced end-systolic circumferential ventricular stress by 39% in dogs with pacing tachycardia-induced heart failure. [22] However, those calculations were done with the Young-LaPlace's law and we have shown that calculation of ventricular stress with the finite element method is more accurate. [16]

PPM relocation [6] and the Coapsys device are unique in that the trans-ventricular strut and mitral repair both serve to reduce end-diastolic fiber stress. It will be interesting to see if patients treated with Coapsys have a sustained reduction in ventricular volume. [12]

### The importance of residual stress

Residual stress is stress that remains when intra-ventricular or intra-vascular pressure is removed. [23] Residual stress, which is present in the normal dog ventricle [24], is thought to be decreased in the dilated LV. In fact, an increase in residual stress was hypothesized by Kresh and Wechsler to be a mechanism whereby pump function was improved after surgical ventricular remodeling. [25] Although our previous finite element simulation of surgical remodeling failed to show an effect of residual stress [26], the results of the current study clearly show a residual stress effect.

Similar to our previous work [13, 14], the POST-OP FE model above assumes that the ventricular wall was stress free at the time of early diastolic filling. To specify residual stress in the POST-OP model requires *a priori* knowledge of the residual stress, which can be measured through destructive *ex vivo* experiments only and is thus impossible with the current *in vivo* study. In contrast and as seen in Figure 4, virtual Coapys was applied to the unloaded PRE-OP model thereby generating residual stress. Although there was close approximation between VIRTUAL-COAPSYS and POST-OP models, VIRTUAL-COAPSYS did fail to consider any potential remodeling occurring in the 2 weeks after device application. However, we believe that the difference in stress calculation between the two models is primarily due to the addition of residual stress to the VIRTUAL-COAPSYS model.

### Effect of Coapsys on pump function

We found that Coapsys implantation shifted EDPVR further to the left than ESPVR on the pressure-volume diagram. This is the same pattern seen with other surgical remodeling procedures including Myocor Myosplint [27], adjustable passive constraint [13] and the Dor procedure. [14] In each of those procedures, pump function (stroke volume/ LV ED pressure relationship) was decreased. With the Coapsys device, however, the decrease in pump function is accompanied by the concomitant elimination of mitral regurgitation. This

elimination compensates for the decrease in total stroke volume by maintaining the forward stroke volume, and thus overall pump function is intact.

It should be noted that our analysis suggests that contractility in the remote myocardium was reduced 2 weeks after CABG/ Coapsys. The mechanism for this reduction is unclear. However, it is worth noting that if post-operative contractility returns to baseline late after Coapsys application, our model predicts that stroke volume would increase by 12 ml at an end-diastolic pressure of 20 mmHg. In the future, it will be important to image post-operative patients at times greater than two weeks after the Coapsys procedure.

### Study limitations

Calculation of regional myocardial material properties is ideally done by comparing calculated regional deformation or strain with measured values. [18, 28] Unfortunately, the magnetic resonance images obtained in this study did not include measures of regional strain. As a consequence, estimates of regional material properties were less accurate.

Pre and post operative LV end-diastolic pressures were estimated from pulmonary artery pressures obtained during general anesthesia and are therefore probably an under-estimate. Also, the model did not include the infarct borderzone, mitral valve, papillary muscles or right ventricle. Also, we plan to include a mathematical lumped parameter model of the systemic and pulmonary circuits in the future. This will more accurately simulate the complex afterload associated with mitral regurgitation.

## Conclusions and Future Directions

The Coapsys device decreases myofiber stress at ED and ES. In addition, because it also treats mitral regurgitation, pump function is maintained. The reduction in myofiber stress may contribute to the long term effect of Coapsys on LV remodeling.

Future studies should include magnetic resonance imaging-based measures of regional function so that myocardial material properties can be properly optimized. In addition, late imaging time points should be included to determine if the effect on LV volume is stable and to see if contractility returns to pre-operative levels late after Coapsys. Hopefully, in the future computational modeling will be able to be used to determine the mechanical effect of operations and devices designed to treat heart failure before animal and human studies are started.

## Acknowledgments

This study was supported by NIH grants R01-HL084431 (Dr. Ratcliffe), R01-HL077921 (Dr. Guccione) and R01-HL086400 (Dr. Guccione). Richard Carrick was supported by a Summer Research Fellowship from the University of Vermont. This support is gratefully acknowledged.

## References

1. De Bonis M, Lapenna E, Verzini A, et al. Recurrence of mitral regurgitation parallels the absence of left ventricular reverse remodeling after mitral repair in advanced dilated cardiomyopathy. Ann Thorac Surg. 2008; 85(3):932–9. [PubMed: 18291174]
2. Hung J, Papakostas L, Tahta SA, et al. Mechanism of recurrent ischemic mitral regurgitation after annuloplasty: continued LV remodeling as a moving target. Circulation. 2004; 110(11 Suppl 1):II85–90. [PubMed: 15364844]
3. Magne J, Pibarot P, Dagenais F, et al. Preoperative posterior leaflet angle accurately predicts outcome after restrictive mitral valve annuloplasty for ischemic mitral regurgitation. Circulation. 2007; 115(6):782–91. [PubMed: 17283262]

4. Matsunaga A, Tahta SA, Duran CM. Failure of reduction annuloplasty for functional ischemic mitral regurgitation. J Heart Valve Dis. 2004; 13(3):390–7. discussion 397-8. [PubMed: 15222285]
5. McGee EC, Gillinov AM, Blackstone EH, et al. Recurrent mitral regurgitation after annuloplasty for functional ischemic mitral regurgitation. J Thorac Cardiovasc Surg. 2004; 128(6):916–24. [PubMed: 15573077]
6. Kron IL, Green GR, Cope JT. Surgical relocation of the posterior papillary muscle in chronic ischemic mitral regurgitation. Ann Thorac Surg. 2002; 74(2):600–1. [PubMed: 12173864]
7. Langer F, Kunihara T, Hell K, et al. RING+STRING: Successful repair technique for ischemic mitral regurgitation with severe leaflet tethering. Circulation. 2009; 120(11 Suppl):S85–91. [PubMed: 19752391]
8. Langer F, Schafers HJ. RING plus STRING: papillary muscle repositioning as an adjunctive repair technique for ischemic mitral regurgitation. J Thorac Cardiovasc Surg. 2007; 133(1):247–9. [PubMed: 17198821]
9. Grossi EA, Woo YJ, Schwartz CF, et al. Comparison of Coapsys annuloplasty and internal reduction mitral annuloplasty in the randomized treatment of functional ischemic mitral regurgitation: impact on the left ventricle. J Thorac Cardiovasc Surg. 2006; 131(5):1095–8. [PubMed: 16678595]
10. Mishra YK, Mittal S, Jaguri P, Trehan N. Coapsys mitral annuloplasty for chronic functional ischemic mitral regurgitation: 1-year results. Ann Thorac Surg. 2006; 81(1):42–6. [PubMed: 16368332]
11. Mittal S, Mishra Y, Trehan N. Coapsys® Leads to Global Reversal of Left Ventricular Remodeling: Expanded TRACE Study Analysis. Circulation. 2007; 116:II–373.
12. Grossi E, Patel N, Woo Y, et al. Outcomes of the Randomized Evaluation of a Surgical Treatment for Off-pump Repair of the Mitral Valve (RESTOR-MV) Trial. J Am Coll Cardiol. 2010; 55(suppl 1):E1366.
13. Jhun CS, Wenk JF, Zhang Z, et al. Effect of adjustable passive constraint on the failing left ventricle: a finite-element model study. Ann Thorac Surg. 2010; 89(1):132–7. [PubMed: 20103222]
14. Sun K, Zhang Z, Suzuki T, et al. Dor procedure for dyskinetic anteroapical myocardial infarction fails to improve contractility in the border zone. J Thorac Cardiovasc Surg. 2010; 140(1):233–9. 239 e1-4. [PubMed: 20299030]
15. Kerckhoffs RC, Lumens J, Vernooy K, et al. Cardiac resynchronization: insight from experimental and computational models. Prog Biophys Mol Biol. 2008; 97(2-3):543–61. [PubMed: 18417196]
16. Zhang Z, Tendulkar A, Sun K, et al. Comparison of the Young-Laplace law and finite element based calculation of ventricular wall stress: implications for postinfarct and surgical ventricular remodeling. Ann Thorac Surg. 2011; 91(1):150–6. [PubMed: 21172505]
17. Walker JC, Ratcliffe MB, Zhang P, et al. Magnetic resonance imaging-based finite element stress analysis after linear repair of left ventricular aneurysm. J Thorac Cardiovasc Surg. 2008; 135(5): 1094–102. 1102 e1-2. [PubMed: 18455590]
18. Sun K, Stander N, Jhun CS, et al. A computationally efficient formal optimization of regional myocardial contractility in a sheep with left ventricular aneurysm. J Biomech Eng. 2009; 131(11): 111001. [PubMed: 20016753]
19. Wenk JF, Zhang Z, Cheng G, et al. First finite element model of the left ventricle with mitral valve: insights into ischemic mitral regurgitation. Ann Thorac Surg. 2010; 89(5):1546–53. [PubMed: 20417775]
20. Sunagawa K, Maughan WL, Burkhoff D, Sagawa K. Left ventricular interaction with arterial load studied in isolated canine ventricle. Am J Physiol. 1983; 245(5 Pt 1):H773–80. [PubMed: 6638199]
21. Starling MR. Effects of valve surgery on left ventricular contractile function in patients with long-term mitral regurgitation. Circulation. 1995; 92(4):811–8. [PubMed: 7641361]
22. McCarthy PM, Takagaki M, Ochiai Y, et al. Device-based change in left ventricular shape: a new concept for the treatment of dilated cardiomyopathy. J Thorac Cardiovasc Surg. 2001; 122(3):482–90. [PubMed: 11547298]
23. Fung, YC. Biomechanics: Motion, flow, stress, and growth. Springer Verlag; New York: 1990.

24. Rodriguez EK, Omens JH, Waldman LK, McCulloch AD. Effect of residual stress on transmural sarcomere length distributions in rat left ventricle. Am J Physiol. 1993; 264(4 Pt 2):H1048–56. [PubMed: 8476082]

25. Kresh JY, Wechsler AS. Heart reduction surgery can reconstitute the residual stress-strain state of the left ventricle. J Thorac Cardiovasc Surg. 1998; 116(6):1084–6. [PubMed: 9832707]

26. Guccione JM, Moonly SM, Wallace AW, Ratcliffe MB. Residual stress produced by ventricular volume reduction surgery has little effect on ventricular function and mechanics: a finite element model study. J Thorac Cardiovasc Surg. 2001; 122(3):592–9. [PubMed: 11547315]

27. Ratcliffe MB, Hong J, Salahieh A, Ruch S, Wallace AW. The effect of ventricular volume reduction surgery in the dilated, poorly contractile left ventricle: a simple finite element analysis. J Thorac Cardiovasc Surg. 1998; 116(4):566–77. [PubMed: 9766584]

28. Wenk JF, Sun K, Zhang Z, et al. Regional left ventricular myocardial contractility and stress in a finite element model of posterobasal myocardial infarction. J Biomech Eng. 2011; 133(4):044501. [PubMed: 21428685]

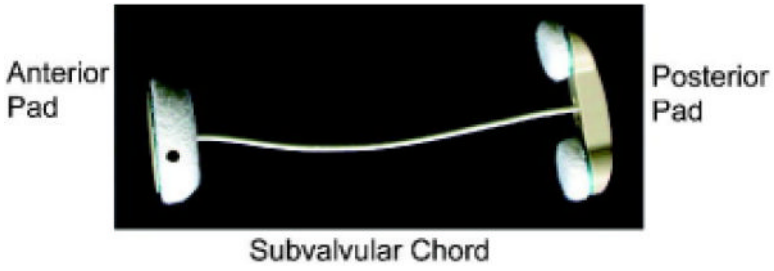


**Figure 1.**
Coapsys device

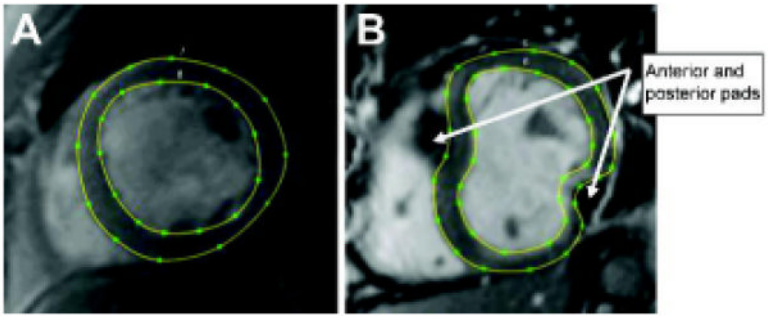


**Figure 2.**
Contoured short-axis cardiac MR images before (A) and after (B) surgical implantation of the Coapsys device. The contours from multiple short-axis images covering the LV from apex to base were used to create patient-specific 3D finite element models.

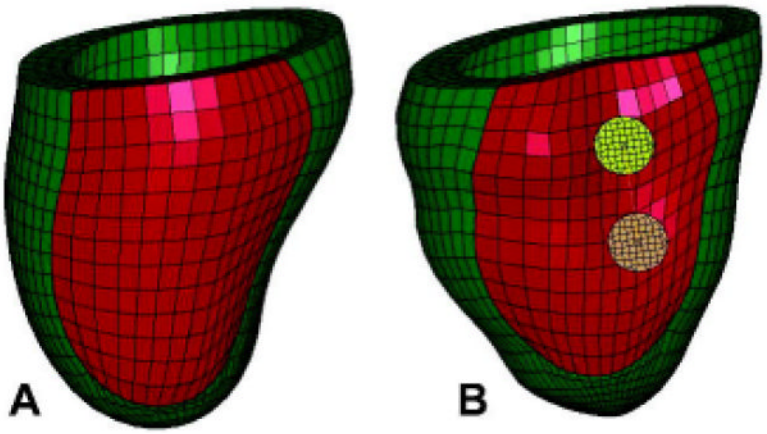


**Figure 3.**
Two views of the unloaded post-Coapsys finite element model showing (A) the PRE-OP model and (B) the COAPSY SUBACUTE model showing the double pad side of the device. Infarct regions are colored with red while the remote regions are colored with green.

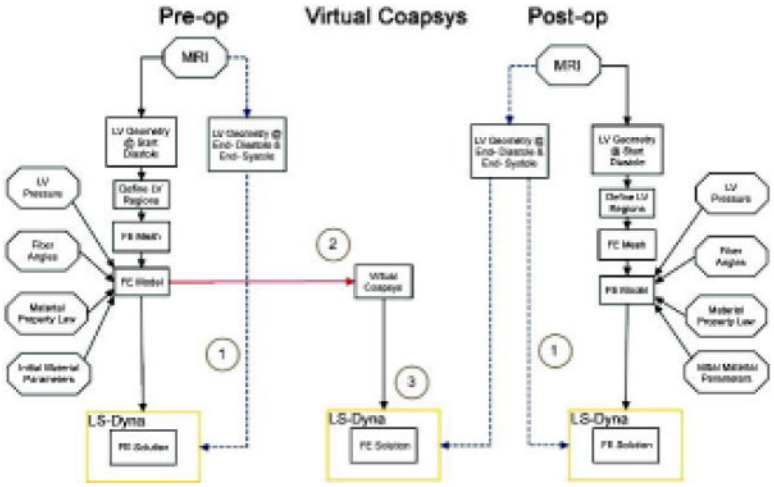


**Figure 4.**

Schematic of FE model development. 1 = determination of diastolic and systolic material parameters by comparison of experimental and computationally derived end-diastolic and end-systolic volume. 2 = the acute mechanical effect of Coapsys (VIRTUAL-COAPSYS:ACUTE). 3 = the effect of residual stress (Comparison between VIRTUAL-COAPSY: SUBACUTE and POST-OP models).

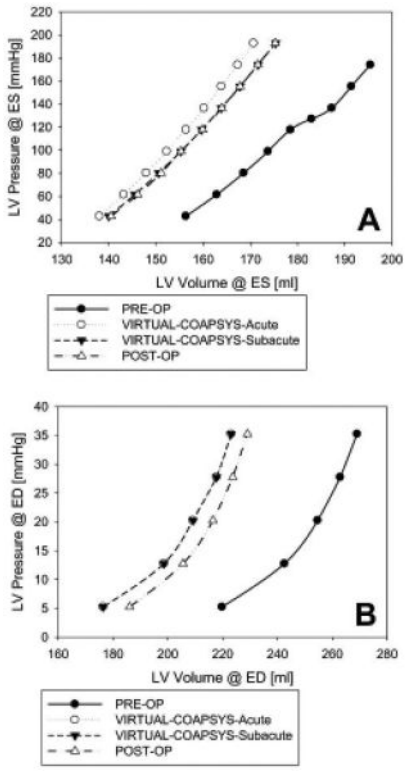


**Figure 5.**
End-systolic (A) and end-diastolic (B) pressure-volume relationship for all four finite element model simulations.

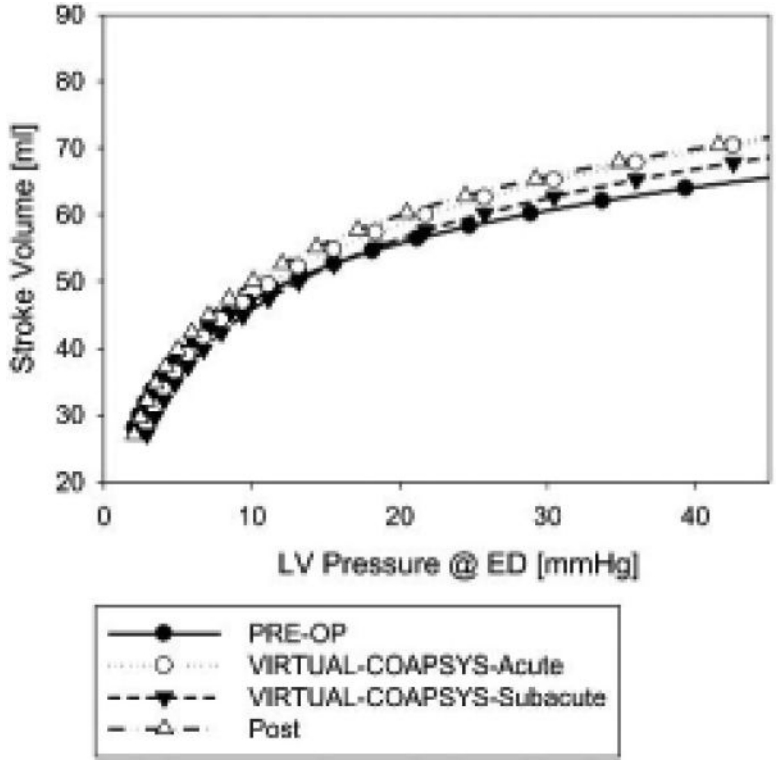


**Figure 6.**
Stroke volume versus end-diastolic pressure relationship for all four finite element model simulations.

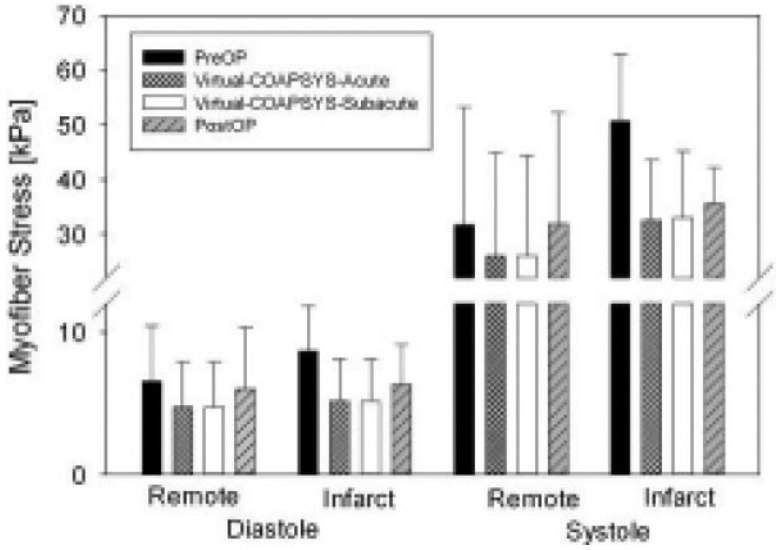


**Figure 7.**
Average end-diastolic and end-systolic myofiber stress in infarct and remote LV regions for all four finite element model simulations.

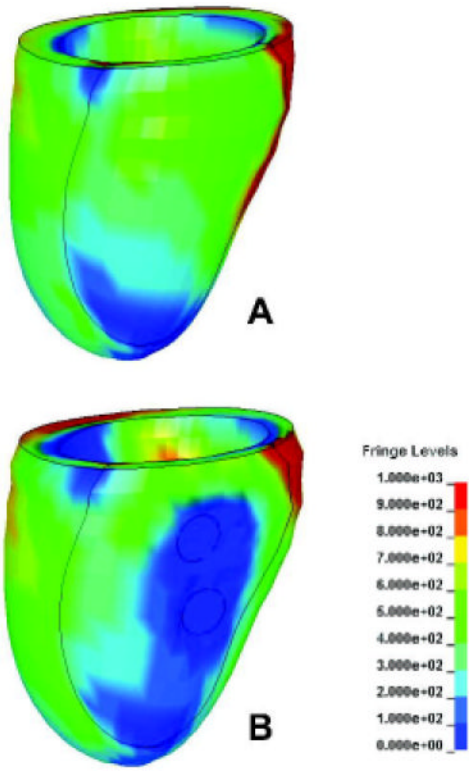


**Figure 8.**
Myofiber stress at ES. (a) PRE-OP model; (b) VIRTUAL-COAPSYS:SUBACUTE model. Unit: kPa.

**Table 1**

**Comparison between input data and finite element model results**

| | Pre op | | | Post op | | | VIRTUAL COAPSYS: SUBACUTE | |
|---|---|---|---|---|---|---|---|---|
| | **Data** | **FE model** | **Difference [%]** | **Data** | **FE model** | **Difference [%]** | **FE model** | **Difference [%]** |
| **LVP at ED [mm Hg]** | 20 | 20 | 0% | 20 | 20 | 0% | 20 | 0% |
| **LVP at ES [mm Hg]** | 118 | 118 | 0% | 115 | 118 | 3% | 118 | 3% |
| **LV Volume at ED [ml]** | 255.6 | 254.7 | 0.3% | 214.9 | 216.5 | 0.7 % | 210.8 | 2.3% |
| **LV Volume at ES [ml]** | 180.56 | 178.49 | 1.1% | 159.4 | 159.9 | 0.3% | 158.1 | 0.8% |

ED - end diastole, ES - end systole, LVP – left ventricular pressure. Note that the VIRTUALCOAPSYS: SUBACUTE model is compared to the POST-OP data column.

*Ann Thorac Surg*. Author manuscript; available in PMC 2013 June 01.

**Table 2**

**Hemodynamic measurements during Coapsys procedure**

| | After sternotomy | After CABG | During Coapsys | After Coapsys (before sternotomy closure) | After Sternotomy closure |
|---|---|---|---|---|---|
| **Heart rate [Beats / minute]** | 60 | 67 | 67 | 89 | 51 |
| **Arterial pressure [mm Hg]** | 118/48 | 107/52 | 102/51 | 99/52 | 115/55 |
| **PAP [mm Hg]** | 38/20 | 35/17 | 29/15 | 32/19 | 35/20 |
| **CVP [mm Hg]** | 10 | 6 | 5 | 5 | 5 |
| **Cardiac output** | 3.2 | 2.7 | 2.4 | | 2.7 |
| **MR Grade** | 3 | 3 | | 1 | |
| **% Coapsys tightening** | NA | NA | 25% | 40% | 40% |

CVP – Central venous pressure, PAP – Pulmonary artery pressure.

## Table 3

**The passive and active LV wall material property used in the current work**

| | C (kPa) | Tmax (kPa) |
|---|---|---|
| **PRE-OP and VIRTUAL-COAPSYS:ACUTE** | 0.196 | 390 |
| **POST-OP and VIRTUAL-COAPSYS:SUBACUTE** | 0.196 | 330 |